*Cryosphere*

Supporting Information for:

*Impact of glacial isostatic adjustment on zones of potential grounding line stability in the Ross Sea Embayment (Antarctica) since the Last Glacial Maximum*

**Samuel T. Kodama[1], Tamara Pico[1], Alexander A. Robel[2], John Erich Christian[3], Natalya Gomez[4], Casey Vigilia[5], Evelyn Powell[6], Jessica Gagliardi[1], Slawek Tulaczyk[1], Terrence Blackburn[1]**

[1]Earth and Planetary Science, University of California-Santa Cruz, Santa Cruz, CA, USA
[2] School of Earth and Atmospheric Sciences, Georgia Institute of Technology, Atlanta, GA, USA
[3]Department of Earth Sciences, University of Oregon, Eugene, OR, USA
[4] Earth and Planetary Sciences, McGill University, Montreal, Quebec, Canada
[5]Jackson School of Geosciences, University of Texas at Austin, Austin, TX, USA
[6] Lamont-Doherty Earth Observatory of Columbia University, Palisades, NY, USA

**Contents of this file:**
**Text**
- S1. Alternative Earth rheology models
- S2. Flowline modeling
- S3. Continental shelf edge emergent potential zones of grounding line stability

**Table**
- S1. Parameters used in flowline modeling

**Figures**
- S1. Total deglacial changes in ice sheet volume for each ice history
- S2. Flowline Modeling grounding line flux
- S3. No Northern Hemisphere ice sheet growth sensitivity test
- S4. Number of "emergent" zones of potential stability through time
- S5. Stable grounding line elevations as a function of distance downstream from ice divide and accumulation, ice shelf buttressing, and basal friction
- S6. Relative sea level curve for offshore Northern Victoria Land
- S7. Alternate Earth rheology model sensitivity test
- S7. Main text Figure 5 with Gol14 ice history
- S8. Main text Figure5 with W12 ice history

**Supplementary Material**
S1. Alternate Earth rheology models
        To test the sensitivity of our results to the choice of Earth model, we simulate glacial isostatic adjustment W12 and Gol14 using an Earth model characterized by a 50 km lithosphere and low viscosity zone of $10^{19}$ Pa·s from 50 km to 200 km depth, viscosity of 2 x $10^{20}$ Pa·s from 200 km to 670 km depth, and lower mantle viscosity of 30 x $10^{20}$ Pa·s. For the Gom18 ice history we explore sensitivity to Earth model by comparing to the 1-D reference Earth model, which has an upper mantle viscosity ~1-2 orders of magnitude higher than the 3D earth model (Gomez et al., 2018 their Figure 1).

When we perform our grounding line stability analysis using changes in topography simulated with the above alternate Earth models, we find that the results are broadly similar (Figure S7). The largest difference is a greater increase in "emergent" zones of potential stability within the interior of the Ross Sea Embayment for all three ice histories, particularly for W12 and Gol14, as well as an increase in areas that are more stable at present day than at the last glacial maximum (Figure S7, red zones).

S2. Flowline modeling

To validate our simple model of grounding line stability we run a 1-D marine ice sheet evolution, shallow-shelf approximation, flowline model (Robel, 2021) over a representative ice stream path. We use a flowline model based off of the grounding line treatment from Schoof (2007) which has been benchmarked by modeling grounding line flux over a synthetic bed (Schoof 2007, Equation 10). Although the simple model of grounding line stability can efficiently test grounding line stability for a large ensemble of parameters, it does not account for ice flow aspects such as glacier velocity, ice thickness profiles, and interactions with upstream topography. The transient flowline model allows us to account for these variables and test if similar trends in grounding line behavior are observed in a more comprehensive model. Since the flowline model transiently evolves, a "steady-state" is not achieved, and we instead record trends in grounding line flux and retreat rate.

We test the impact of glacial isostatic adjustment-induced changes in topography on grounding line retreat by first solving for a steady-state ice profile with the grounding line located at the edge of the continental shelf, similar to the Last Glacial Maximum position of the flowline. The initial condition for the transient flowline run is a steady-state ice stream profile for both present-day (rebounded) and 20 ka (isostatically depressed) topographies. During the first timestep of transient run, surface mass balance is step-decreased from 0.42 m/yr to -0.042 m/yr for all (present-day and 20 ka) model runs. Surface mass balance is then held constant at -0.042 m/yr for the remainder of the modeling time, and the model is run until the grounding line reaches the present-day grounding line position.

Input parameters of basal friction and ice shelf buttressing used for the flowline modeling are within the range of values used in the simple approximation used in the main text, while an initial average upstream surface mass balance above the range of values used in the main text was required to achieve a steady-state position on the edge of the continental shelf. Although the initial average upstream surface mass balance value is larger than the range of values used in the simple approximation used in the main text, the initial value and step change is the same for all modeling scenarios (present-day and 20), and therefore we can still isolate the role of glacial isostatic adjustment in grounding line retreat.

The ice stream flowline modeling results broadly agree with our analysis using the simple grounding line approximation in the main text. We interpret locations with smaller grounding line discharge and slower retreat rates as more "stable" (similar to our potential zones of stability in the main text). The simple grounding line stability model (main text) predicts grounding line stability in locations where grounding line retreat rate, and discharge are at a minimum for the Gom18 ice history (1,400–1,600 km and ~800 km downstream) and near the edge of the continental shelf for W12 and Gol14 (1,400–1,600 km downstream; Figure S5). The simple

grounding line stability model (main text) also predicts some potential stable grounding line zones for present-day topography and no potential stable grounding line zones for 20 ka paleotopography in locations where grounding line retreat rates for present-day topography are roughly an order of magnitude less than for 20 ka paleotopographies (900–1,400 km downstream; Figure S5).

S3. Continental shelf edge emergent potential zones of grounding line stability

A small area of emergent potential zones of grounding line stability is located on a large submarine bank near the edge of the continental shelf (Main text Figure 1e and Figure 3) despite this area undergoing a sea-level rise since 20 ka. At 20 ka, the depth of this bank is shoaled due to uplift of the peripheral bulge, such that we predict positive mass balance (resulting in grounding line advance) for grounding line locations on this shoaled bank. Only once relative sea level at the bank increases, due to peripheral bulge collapse, can grounding line fluxes be balanced to produce a numerical "steady state". This reason for emergent potential zones of grounding line stability is also the reason for the percent increase in density of potential zones of grounding line stability in the surrounding areas.

**Supplementary Table**

| STable 1: Parameters used in Flowline modeling | |
|---|---|
| Parameter | Value |
| upstream average surface mass balance at $t_0$ ($\frac{m}{yr}$) | 0.1 |
| upstream average surface mass balance at $t_{1\to\infty}$ ($\frac{m}{yr}$) | 0.03 |
| Nye-Glen law coefficient ($Pa^{-n} \cdot s^{-1}$) | 4.227 x $10^{-25}$ |
| Weertman friction law exponent | $\frac{1}{3}$ |
| Nye-Glen law exponent | 3 |
| Basal friction coefficient ($Pa \cdot m^{\frac{-1}{n}} \cdot s^{\frac{1}{n}}$) | 6 x $10^6$ |
| Ice shelf Buttressing parameter | 0.5 |
| Ice density ($\frac{kg}{m^3}$) | 917 |
| Sea water density ($\frac{kg}{m^3}$) | 1028 |

**STable 1 |** Values of parameters used for flowline modeling.

**Supplementary Figures**
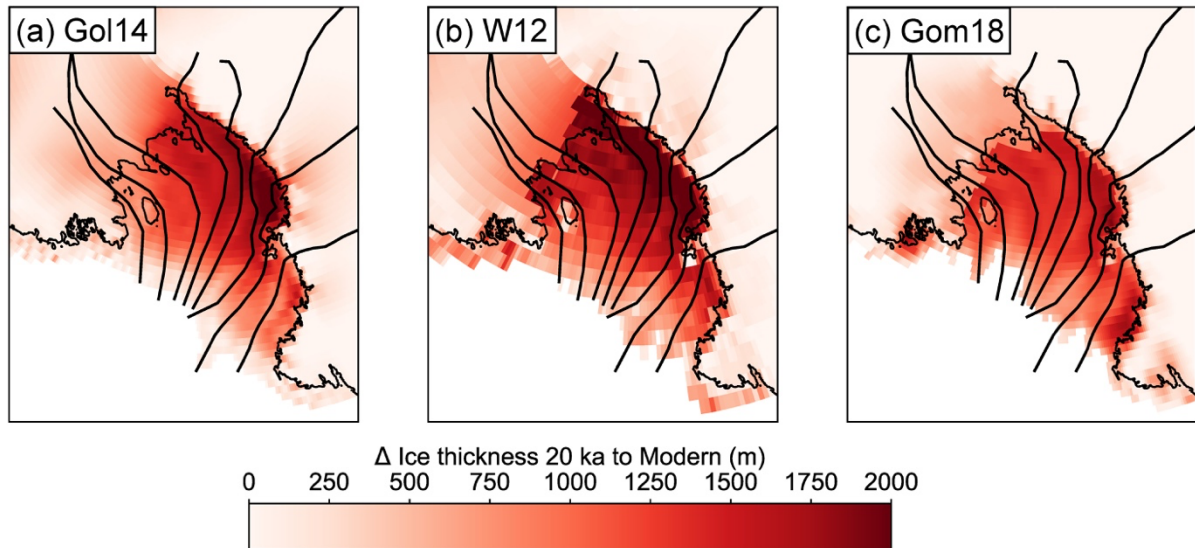
**Figure S1 |** Change in ice thickness since 20 ka in the Ross Sea for a) Gol14, b) W12, and c) Gom18 deglacial histories.
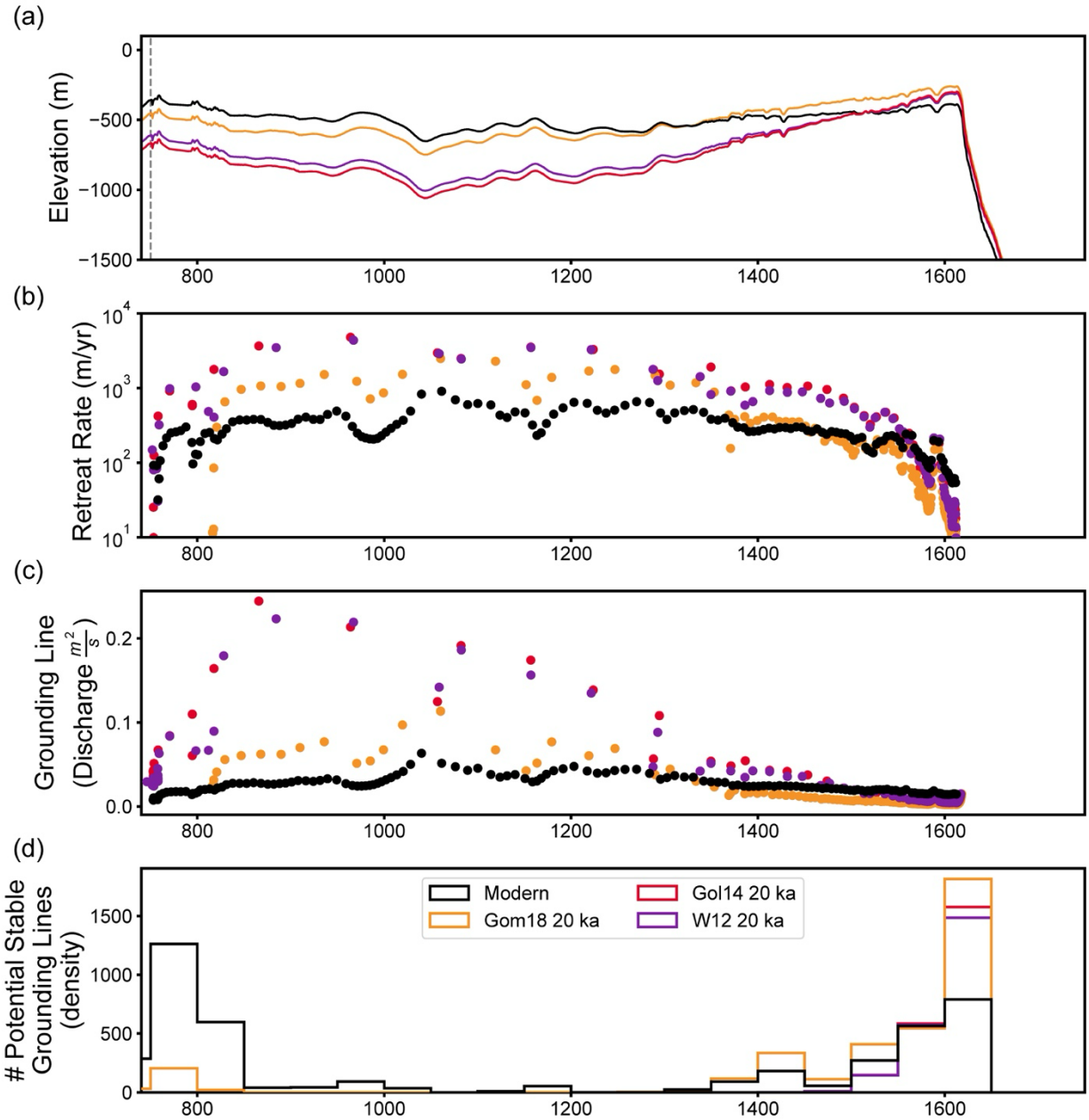
**Figure S2 |** a) Present-day topography (black), and 20 ka paleotopography modeled with W12 (purple), Gol14 (red), and Gom18 (orange). Dashed line is present-day grounding line location. b) Grounding line retreat rate, c) Grounding line discharge, and d) Potential stable grounding line positions simulated using the simple grounding line flux approach described in the main text.
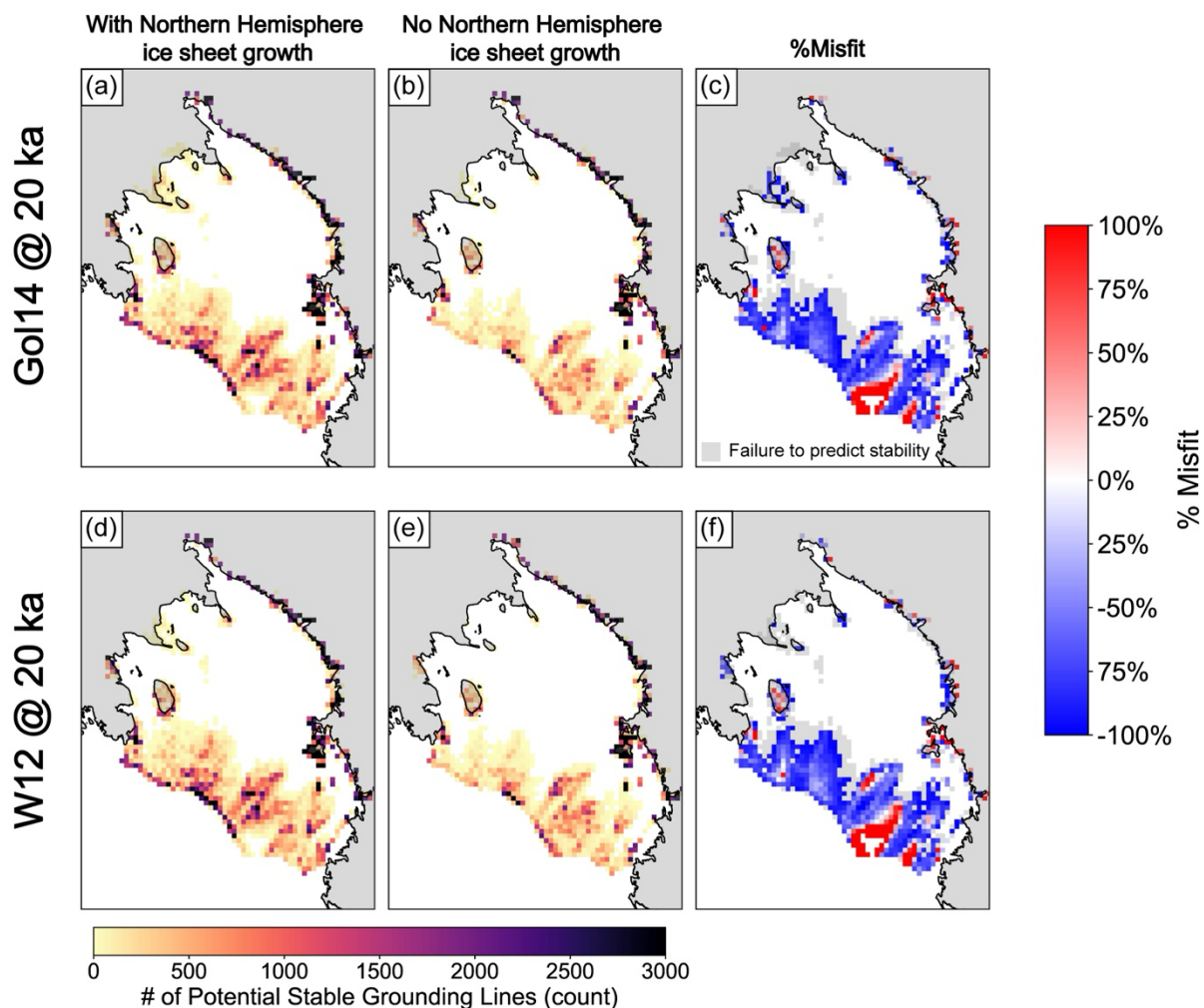
**Figure S3 |** Zones of potential stability for Gol14 ice history with a) growth of Northern Hemisphere (NH) ice sheets b) no growth of Northern Hemisphere ice sheets c) Percent misfit defined as difference of stable grounding line positions calculated with NH ice sheets and no NH ice sheets divided by stable grounding line positions calculated using NH ice sheets $\left(\frac{ZPS_{NH}-ZPS_{no\,NH}}{ZPS_{NH}}\right)$. d-f) same as a-c) but with the W12 ice history.
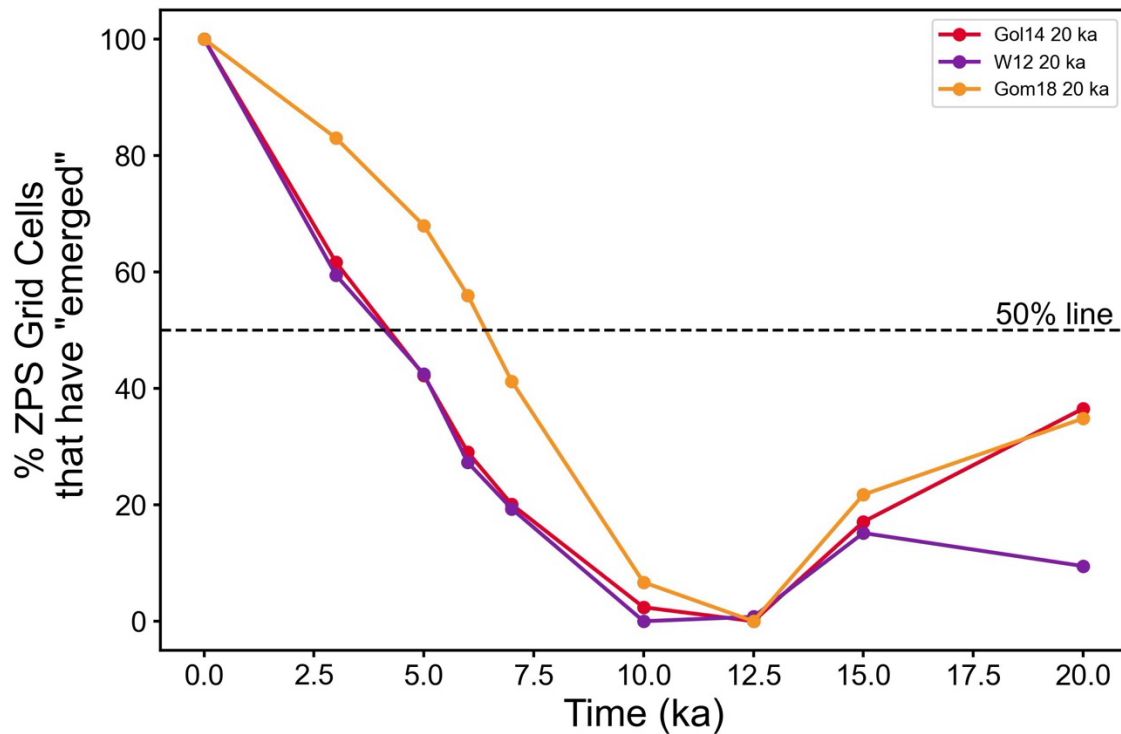
**Figure S4** | Percent of "emergent" zones of potential stability (zones that are stable at present-day but not stable at 20 ka) that have become stable. Dashed line denotes 50%. Some zones of potential stability have already "emerged" at 20 ka because the maximum isostatic depression occurs 12.5-10 ka. From 12.5-10 ka, the depression causes a minimum in zones of potential stability and therefore a maxima in the number of zones of potential stability that are not stable at the current time (12.5-10 ka) but are stable at present-day (and therefore a minima in zones of potential stability that have "emerged").
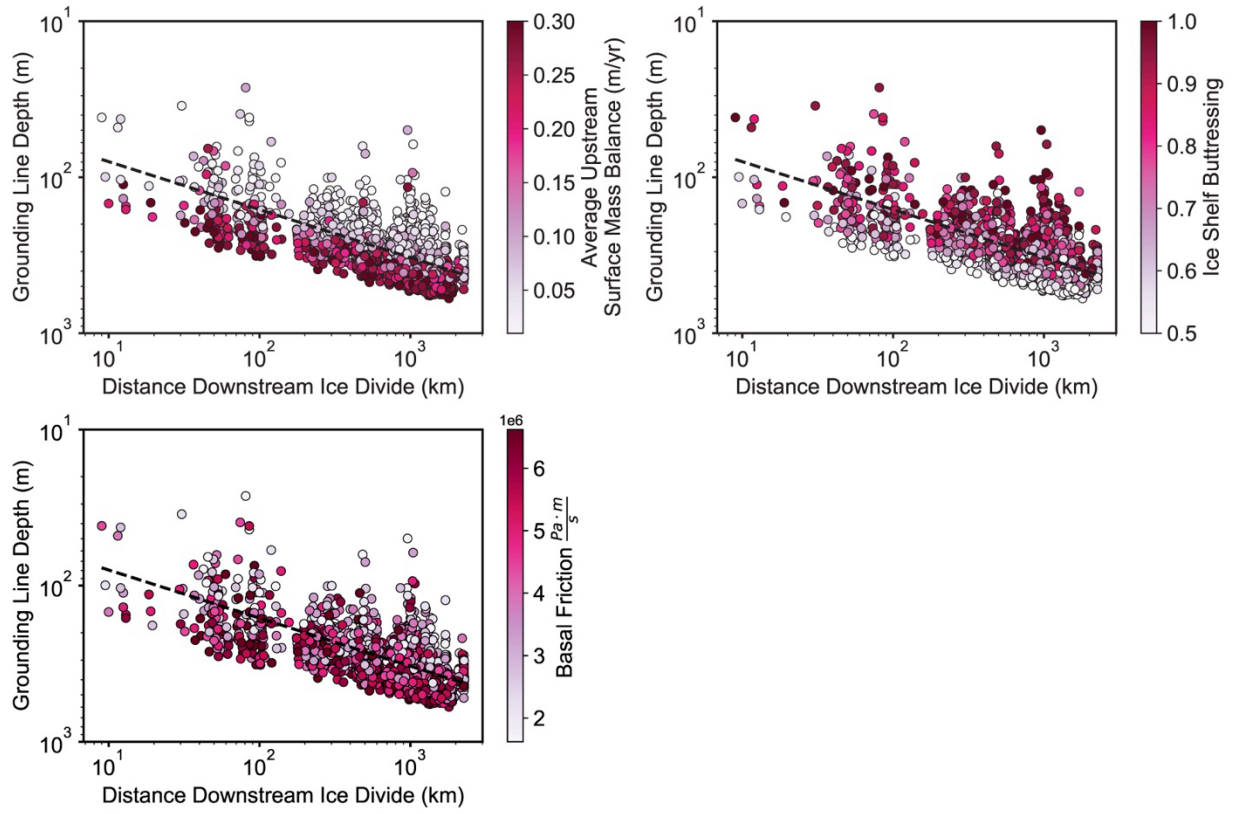
**Figure S5 |** Grounding line depth plotted as a function of distance downstream from the ice divide. Points are colored by a) average accumulation rate, b) ice shelf buttressing coefficient, and c) basal friction coefficient.
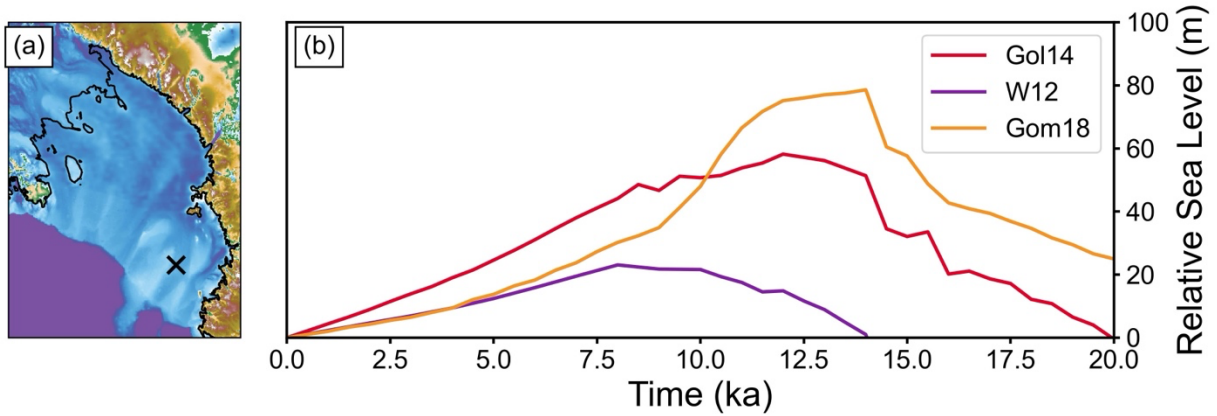
**Figure S6 |** a) Location of relative sea-level history in b) Relative sea level history over the past 20 ka for the Gol14 (red), W12 (purple), and Gom18 (orange) ice histories.

Percent Change in # of
Potential Stable Grounding Lines
20 ka to present

LGM more stable ← → Present-day more stable
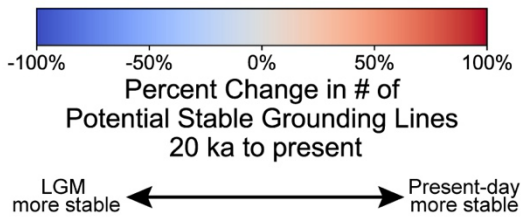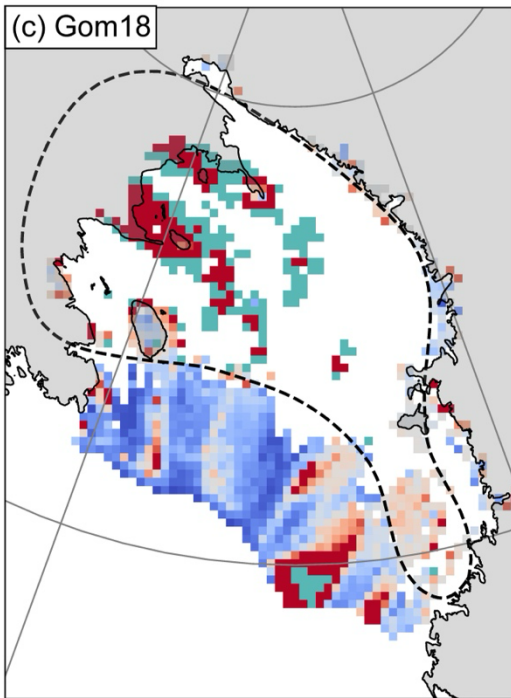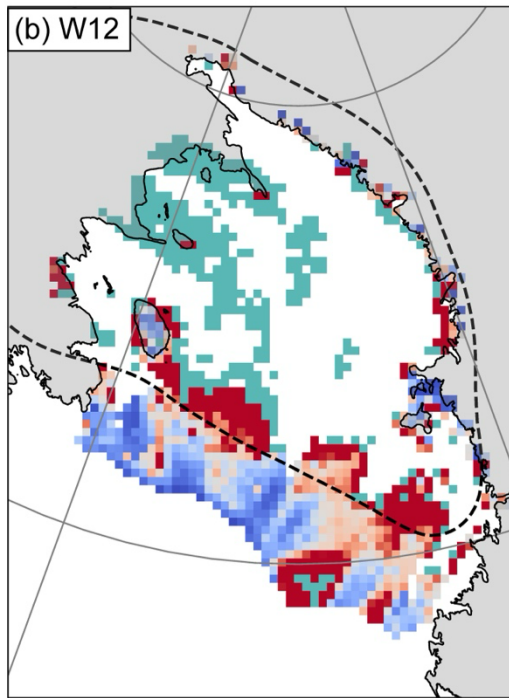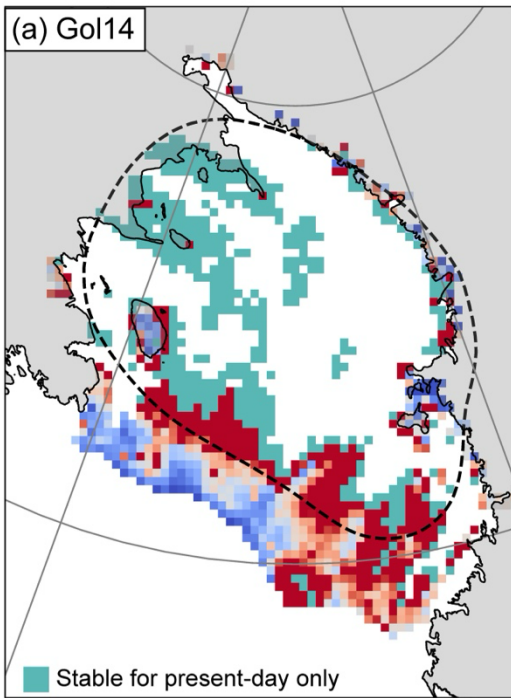
**Figure S7|** Glacial isostatic adjustment-induced percent change in stable grounding line positions across 20 km x 20 km grid cells for entire Ross Sea based on glacial isostatic adjustment simulations using alternate Earth models for a) Gol14, b) W12, and c) Gom18. Grid cells that have stable grounding line positions in the present-day and no stable grounding line positions at 20 ka are outlined by a black line. Thin black line is present-day day grounding line.
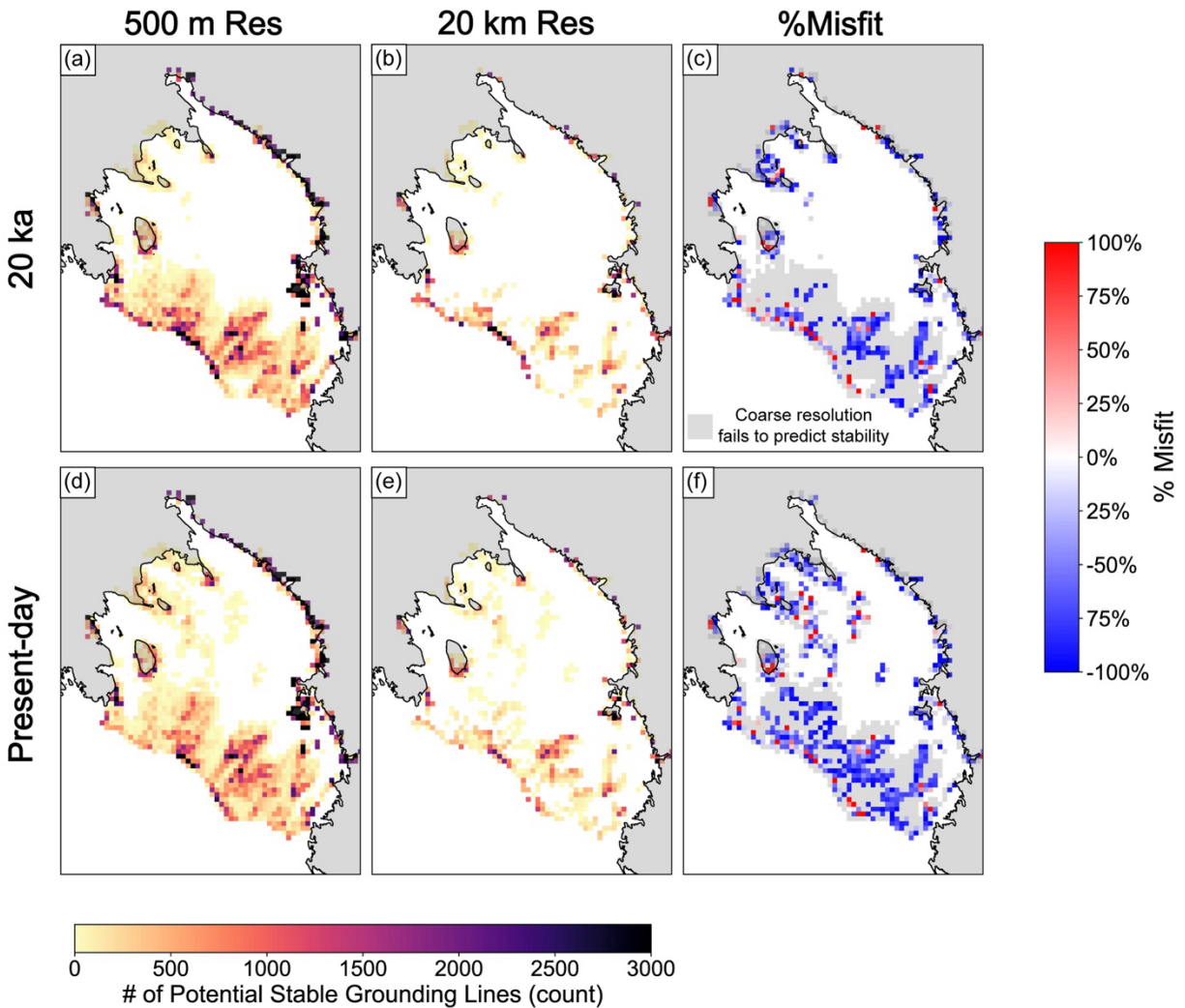
**Figure S8 |** Same as main text Figure 5, but for the Gol14 ice history.
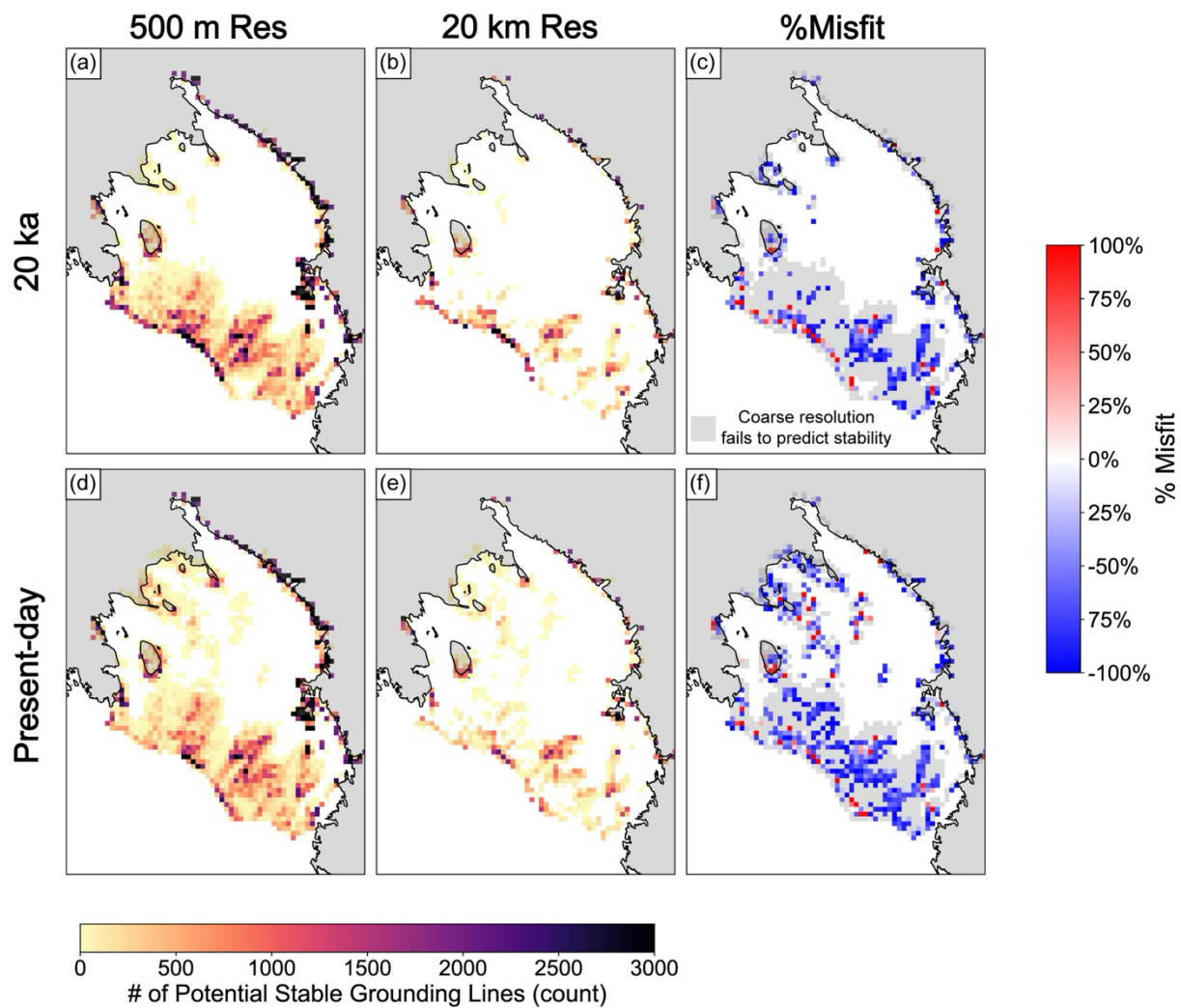
**Figure S9 |** Same as main text Figure 5, but for the W12 ice history.

**References**

Golledge, N. R., Menviel, L., Carter, L., Fogwill, C. J., England, M. H., Cortese, G., and Levy, R. H.: Antarctic contribution to meltwater pulse 1A from reduced Southern Ocean overturning, Nature Communications, 5, https://doi.org/10.1038/ncomms6107, 2014.

Gomez, N., Latychev, K., and Pollard, D.: A coupled ice sheet-sea level model incorporating 3D earth structure: Variations in Antarctica during the Last Deglacial Retreat, Journal of Climate, 31, 4041–4054, https://doi.org/10.1175/JCLI-D-17-0352.1, 2018.

Robel, A., A.: SSAsimpleM, 2021.

Schoof, C.: Ice sheet grounding line dynamics: Steady states, stability, and hysteresis, Journal of Geophysical Research: Earth Surface, 112, https://doi.org/10.1029/2006JF000664, 2007.

Whitehouse, P. L., Bentley, M. J., and Le Brocq, A. M.: A deglacial model for Antarctica: Geological constraints and glaciological modelling as a basis for a new model of Antarctic glacial isostatic adjustment, Quaternary Science Reviews, 32, 1–24, https://doi.org/10.1016/j.quascirev.2011.11.016, 2012.